Power-law scattering in fluids with a nonscalar order parameter

Apollo P. Y. Wong, Pierre Wiltzius, Ronald G. Larson, and Bernard Yurke
AT&T Bell Laboratories, Murray Hill, New Jersey 07974
(Received 30 November 1992)

We studied the coarsening behavior of two lyotropic liquid-crystal systems by static light scattering. The samples were quenched from the isotropic phase into either the nematic phase or a region of coexistence between nematic and isotropic phases. In the coexistence region, we observed, in both two and three dimensions, Porod power-law tails of the scattering intensity. Such a behavior is described by $S(q) \sim q^{-(d+1)}$ in the limit of large wave vectors q, where S is the scattering intensity, q is the wave vector, and d is the dimension of the system. In addition, the nematic phases displayed novel power-law scaling behavior at large q, namely, $S(q) \sim q^{-u}$, where $u=4$ in two dimensions and $u=6$ in three dimensions. These results will be compared to recent theoretical predictions.

PACS number(s): 05.70.Fh, 64.60.−i, 61.30.−v

In x-ray scattering from porous materials with sharp interfaces, Debye, Anderson, and Brumberger concluded as long ago as 1957 that at large wave vector $[q=(4\pi/\lambda)\sin(\theta/2)]$, the structure factor should fall off as q^{-4} [1]. This result was later generalized to include any binary system with sharp interfaces. In this case, the structure factor was expected to obey $S(q) \sim q^{-(d+1)}$, d being the dimension of the system. This is usually called Porod's law [2]; there are ample experimental evidences confirming this behavior for various fluid and magnet systems [3,4].

Very recently, Porod's law was generalized still further to include systems with complicated order parameters [5,6]. It was predicted that, for a system with an n-component vector order parameter, the structure factor should obey $S(q,t) \sim L(t)^d f(qL(t))$ where $L(t)$ is a time-dependent characteristic length and f is a scaling function that asymptotically approaches $f(x) \sim x^{-(d+n)}$ at large x. Therefore, for a system quenched into its ordered phase, the large-q behavior of the structure factor should be $S(q,t) \sim L(t)^d (qL(t))^{-(d+n)}$ and the usual Porod behavior for a phase-separated binary system with a scalar order-parameter is recovered as the special case at $n=1$.

In the case of binary systems, the sharp interfaces between the two components are the dominant scatterers and the characteristic length of the system can then naturally be taken as the characteristic domain size. However, for systems with complicated order parameters, the concepts of domains and domain walls are no longer applicable. The physical meaning of the characteristic length scale is not obvious, although one length scale in the system is related to the defect density. Nevertheless, the results below agree well with the generalized Porod form of scaling which indicates that there is such a characteristic length scale in the nematic regime. Moreover, the sample thickness d^* at which the cross over from two- to three-dimensional behavior occurs is surprisingly large (on the order of tens or hundreds of microns) compared to the "molecular" length scales, which are only on the order of 100 to 2000 Å. Presumably d^* is determined by the characteristic length $L(t)$. We will argue that in the case of a nematic liquid crystal, the dominant source of scattering comes from the disclinations, and that the length scales $L(t)$ and d^* are indeed related to the distance between them.

We report in this article static light-scattering results on two lyotropic liquid-crystalline systems, namely, poly γ-benzyl-glutamate (PBG) in meta-cresol and cesium perfluoro-octanoate (CsPFO) in heavy water. These two lyotropes were chosen because of their slow ordering time scales and their small birefringence in the nematic phase. The birefringence of a typical thermotropic liquid crystal is one to three orders of magnitude higher than that of the above two systems, which makes it difficult to avoid multiple scattering. Moreover, both the PBG and CsPFO systems have been well studied, and their phase diagrams are readily available [7,8]. For the concentrations considered here, both systems have an isotropic phase at high temperatures, a nematic-isotropic coexistence phase in an intermediate temperature range, and they are pure nematic liquid crystals at yet lower temperatures. One difference between the two systems, however, is that the coexistence region of the PBG solution spans approximately 40 °C while that of the CsPFO system is only 0.5 °C wide.

The polymer chains of PBG form rods with lengths of approximately 2000 Å and diameters of approximately 15 Å [8]. On the other hand, the CsPFO molecules form disklike micelles that are about 40 Å thick and 150 Å in diameter [9]. Despite their differences, we show below that both systems display similar generalized Porod scaling behavior in the nematic phase. This provides strong evidence that such a scaling behavior is independent of the molecular details and is a generic property of systems with complicated order parameters.

We employ a new technique for gathering the static light-scattering data in which carefully positioned geometric optical elements project the light scattered between 0° and 40° onto a charge-coupled-device (CCD)

camera for recording. The speed of data collection is limited only by the speed of data communication between the CCD camera and the controlling computer; in our system this limit is about 2 s between each snapshot. The temperature stability is better than 25 mK. The layout of the equipment is given elsewhere in detail [10]. The dimensional crossover behavior of each system was studied by varying the sample thickness. The PBG system displays two-dimensional (2D) behavior in a sample of thickness 50 μm, while the CsPFO system shows 2D behavior for samples thinner than 100 μm.

SYNTHETIC POLYPEPTIDE PBLG/PBDG IN *m*-CRESOL

The chemical formula of PBG is $(—NH—CHR—CO—)_n$ where R is the side chain given by $—(CH_2)_2—COOCH_2—C_6H_5$. PBG chains in a heliogenic solvent such as meta-cresol change from open coils at high temperature to helical rigid rods in the ordered state. Chains synthesized with left-handed chirality are labeled PBLG; those with right-handed chirality are called PBDG. Owing to the helicity, an ordered solution of PBLG or PBDG alone will be cholesteric. To eliminate the cholesteric effects, we use a 50-50 racemic mixture of PBLG and PBDG. We have also studied cholesteric solutions of PBLG alone in *m*-cresol and observed no effect of chirality on the scaling behavior. Only results for the racemic mixture of PBLG and PBDG are presented here.

The PBLG-PBDG sample was prepared by dissolving approximately 12% by weight of the polymers with an average molecular weight of 220 000 in meta-cresol. The solution was then allowed to sit at room temperature to allow for phase separation. After about 3 to 4 days, an interface formed between the polymer-rich nematic phase and the meta-cresol-rich isotropic phase. The polymer-rich phase is the heavier of the two. It was extracted from the solution by pipette as the sample for the measurements. This procedure ensures that the system is a pure nematic liquid crystal at room temperature, which gives us a convenient range of temperatures over which the solution is biphasic. The concentration of the sample was determined later by solvent evaporation to be 12.2±0.2 wt. %. The isotropic-coexistence transition temperature is 75 °C and the coexistence-nematic transition temperature is 35 °C approximately as determined by monitoring the sample between crossed polarizers. In the coexistence region, patches of isotropic regions could be seen dispersed throughout the sample. When the temperature was quenched below the nematic temperature, the typical Schlieren pattern would appear.

The PBLG-PBDG sample was sealed in a glass vial of 1-mm light path and thermally anchored to a temperature-controlled block with a Peltier cooler. It was first annealed at 80 °C, then quenched to 50 °C at a cooling rate of 1.7 °C/min.

Figure 1 shows the structure factor as a function of the wave vector on a log-log scale 21 and 160 min after the quench. The solid line is a fit to the large-q tail of the 21-min result which yields a slope of -4.0 ± 0.3. This is consistent with the usual 3D phase separation obeying

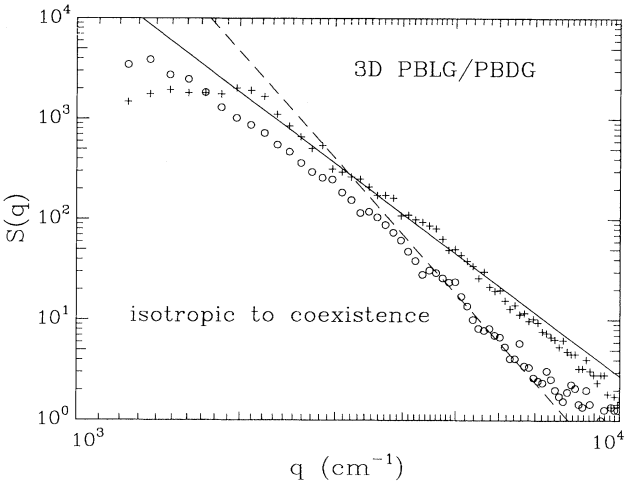

FIG. 1. $S(q)$ vs q for 3D PBG in the coexistence region. The circles are data at 21 min after the quench, and the pluses are data at 160 min after the quench. The solid line is a fit to 21-min data with a slope of -4.0 and the dashed line is a fit to 160-min data with a slope of -6.0.

Porod's law of $S(q)\sim q^{-(d+1)}$ with $d=3$. This suggests that the major source of scattering is from the sharp interfaces between the nematic and isotropic phases. However, at later times, the large-q portion of the data is well fitted by the dashed line of slope -6.0 ± 0.3. This behavior is characteristic for a nematic phase, as shown below. The crossover from a slope of -4 to -6 concurs with the coarsening of the coexisting isotropic and nematic domains. This leads to a decrease of the interfacial area and thus a decrease in the amount of light scattered as predicted by Porod's law.

The 3D nematic behavior of PBLG-PBDG was studied by quenching the sample directly from the isotropic phase at 80 °C into the nematic phase at 20 °C at 1.7 °C/min. Figure 2 shows a typical result of $S(q)$ versus q on a log-log scale in the nematic region. According to the scaling form of the generalized Porod law, $S(q,t)\sim L(t)^d(qL(t))^{-u}$, the data should have an asymptotic slope of $-u$ on a log-log scale. The solid line shown in Fig. 2 is a fit to the large-q part of the data that yields a slope of -6.0 ± 0.3. If one applies the results for the n-component vector model $u=d+n$, then this would suggest that $d=3$ and $n=3$. We will discuss this result later in this article.

The generalized Porod form of the structure factor can be simplified to $S(q,t)\sim L(t)^{-n}q^{-(d+n)}$ so that all the time dependence of the structure factor is originated from the coarsening of the length scale $L(t)$. Therefore, by studying the time dependence of the amplitude, it is possible to obtain information about the coarsening dynamics of the length scale. We fitted the structure factor data to the form of $S(q,t)=A^*q^{-6}$, and the time dependence of A^* is shown in Fig. 3 in log-log scale. The values of A^* have been normalized by the maximum value of A^* in the set. $L(t)$ should grow like $t^{1/2}$ according to previous studies [12]. This implies that the

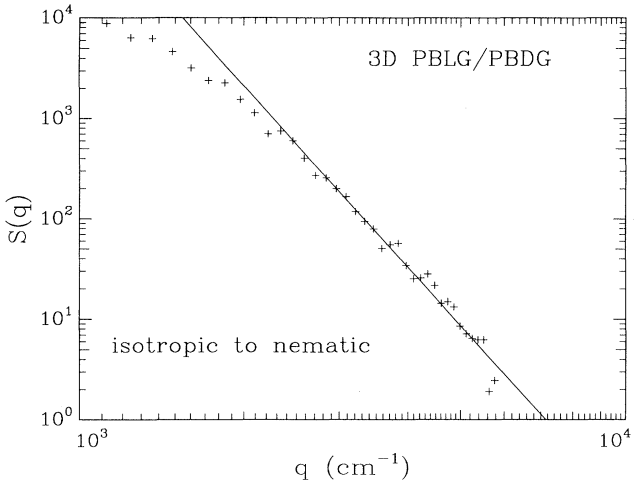

FIG. 2. $S(q)$ vs q for 3D PBG in the nematic region at 53.4 h after the quench to 20 °C. The solid line is a fit with a slope of -6.0.

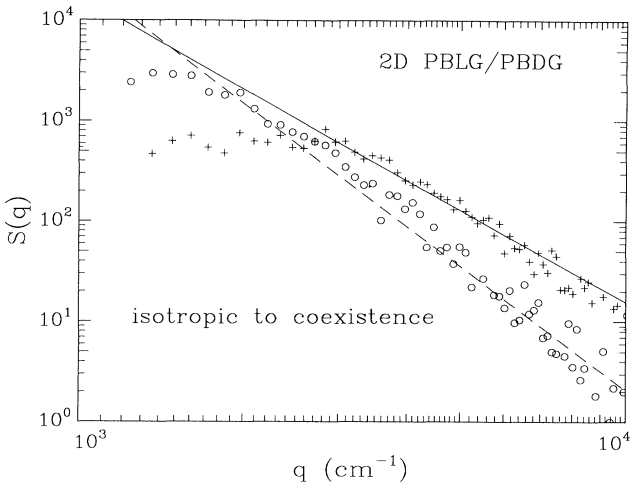

FIG. 4. $S(q)$ vs q for 2D PBLG in the coexistence region. The pluses are data at 3.1 min after the quench, and the circles are data at 10.8 min after the quench. The solid line is a fit to the pluses with a slope of -3.0 and the dashed line is a fit to the circles with a slope of -4.0.

slope on a log-log plot of A^* versus t should have a slope of $-\frac{3}{2}$. The solid line in Fig. 3 denotes a slope of -1.5. Although the data beyond 40 h after the quench seem to approach this power law, it is obvious that the coarsening kinetics of the PBLG-PBDG system are too slow to make the asymptotic time dependence accessible to measurements. In the later part of this article, we will describe experiments on another system where the asymptotic coarsening of $L(t)$ is more readily accessible.

The two-dimensional sample was sealed in a commercially available 50-μm light path quartz cell with a water jacket for temperature control. The sample was quenched from 80 °C into the coexistence region at 60 °C at a rate of 70 °C/min. The structure factors at 3.1 and 10.8 min after the quench are plotted as a function of q in Fig. 4. The solid line is a fit to the large-q region of the 3.1-min data with a slope of -3.1 ± 0.3. The dashed line is a fit to the 10.8-min data with a slope of -4.0 ± 0.3. Similar to the 3D cases, this result indicates that the scattering is caused by interfaces between coexisting domains of isotropic and nematic phases at early times. As the domains coarsen, the interfacial scattering decreases and the late-stage q^{-4} scattering is attributed to the nematic regions.

The q^{-3} behavior observed during the coexistence of nematic and isotropic regions is in agreement with Porod's law for $d=2$. To our knowledge, this is the first

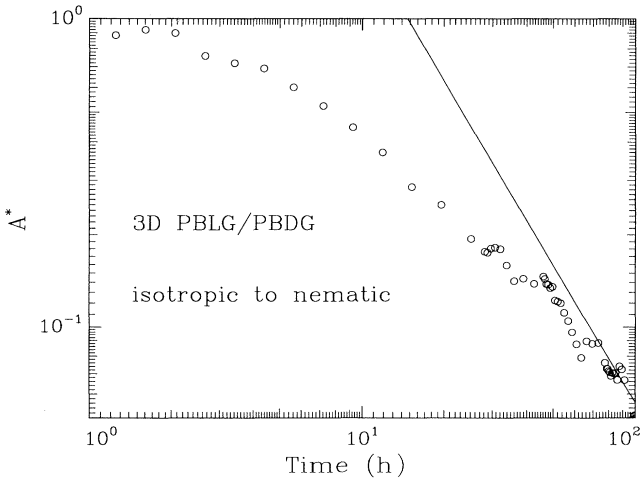

FIG. 3. Amplitude of -6 power-law fit (A^*) vs time for 3D PBLG. The solid line depicts the asymptotic behavior of slope $-\frac{3}{2}$.

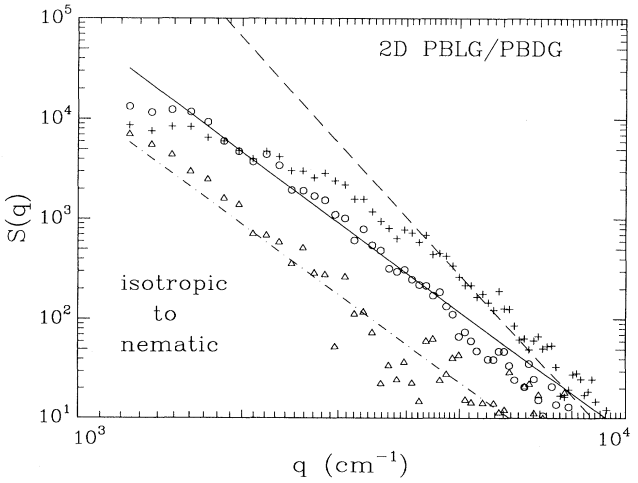

FIG. 5. $S(q)$ vs q for 2D PBG in the nematic region. The pluses, circles, and triangles are data at 10.8, 25.0, and 101.6 min after the quench, respectively. The dashed line is a fit to the pluses with a slope of -6.0. The solid and dotted lines are fits to the circles and triangles. They both have a slope of -4.0.

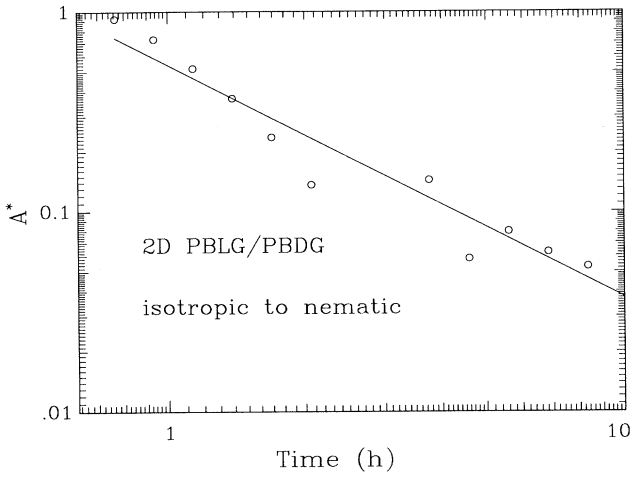

FIG. 6. Amplitude of -4 power-law fit (A^*) vs time for 2D PBLG. The solid line is a fit with slope -1.1.

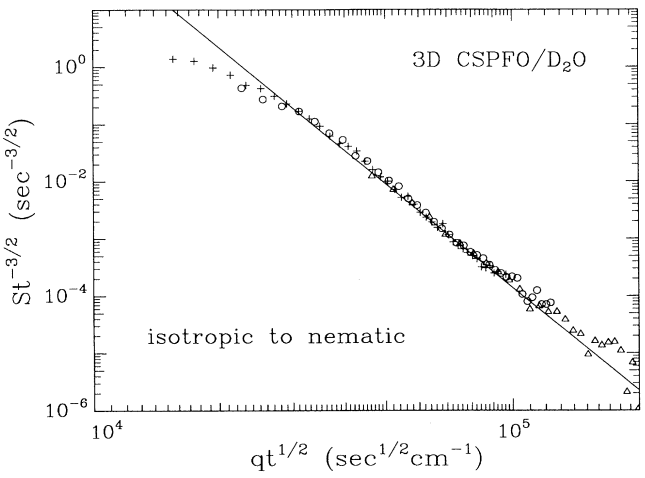

FIG. 7. Scaled form of 3D CsPFO data in the nematic region. The pluses, circles, and triangles are data at 235, 501, and 2097 s after the quench, respectively. The solid line is a fit with slope -6.0.

experimental verification of this power-law behavior in a two-dimensional fluid system.

Similar to the 3D case, the 2D nematic behavior of the sample was studied by directly quenching the sample from the isotropic into the nematic state at 20 °C. However, due to the difference in cell configuration, the quench was at a much faster rate of 70 °C/min. Therefore, it was possible to observe earlier stages of coarsening after the quench than possible with the thicker 3D cell. Figure 5 shows the scattering data for 10.8, 25.0, and 101.6 min after the quench, respectively. The dashed line is a fit to the high-q region at 10.8 min after the quench giving a slope of -6.0 ± 0.3. At such an early stage, the characteristic length scale of the system is small enough compared to the thickness of the sample so that we observe 3D behavior as evidenced by the q^{-6} dependence. As the length scale coarsens, the limited thickness of the sample induces a crossover to 2D behavior as shown by the circles at 25.0 min after the quench. The solid line is a fit with a slope of -4.0 ± 0.3. The dash-dotted line is a fit for the data at an even later time of 101.6 min. It has also a slope of -4.0 ± 0.3. If one applies again the theoretical predictions for the n-component vector model, a slope of -4 implies $d=2$ and $n=2$.

The time dependence of the length scale can also be extracted by fitting the structure factors to the form $S(q)\sim A^*q^{-4}$. A log-log plot of A^* versus time is shown in Fig. 6. The solid line is a fit with slope -1.1 ± 0.2, which is consistent with a length scale growing with $t^{1/2}$, in agreement with theory and simulations [12,13]. It is interesting to note that, in comparison with the 3D system shown in Fig. 3, the 2D system reaches the scaling regime approximately ten times faster.

MICELLES OF CsPFO IN HEAVY WATER

The CsPFO used in this study was prepared by precipitating cesium carbonate ($CsCO_3$) and perfluoro-octanoic acid [CF_3 $(CF_2)_6$ COOH] in a hexane bath. The CsPFO precipitate was dried and recrystallized twice from a bath of a 50-50 mixture of hexane and ethanol by volume. The CsPFO crystal was dissolved in heavy water according to a mass ratio of 1:1.857. The solution made was then filtered with a 0.5-μm teflon filter to remove any solid impurities. The isotropic-to-coexistence transition temperature of this solution is at 28 °C and the coexistence-to-nematic transition temperature is at 27.5 °C.

The 3D nematic behavior of the CsPFO was studied in a sealed sample cell with 1-mm light path. The sample was annealed at 30 °C and then quenched into the nematic phase at 27 °C at a rate of 1.7 °C/min. Typical scattering data are shown in Fig. 7 in a scaled form of $S(q,t)t^{-3/2}$ versus $qt^{1/2}$. This representation of the data

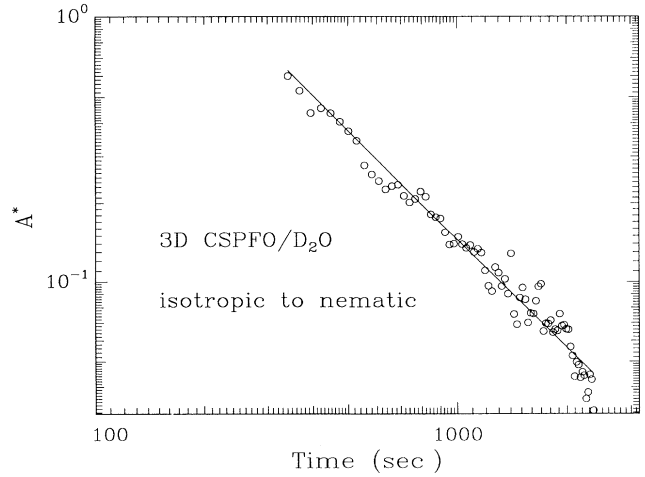

FIG. 8. Amplitude of -6 power-law fit (A^*) vs time for 3D CsPFO. The solid line is a fit with slope -1.4.

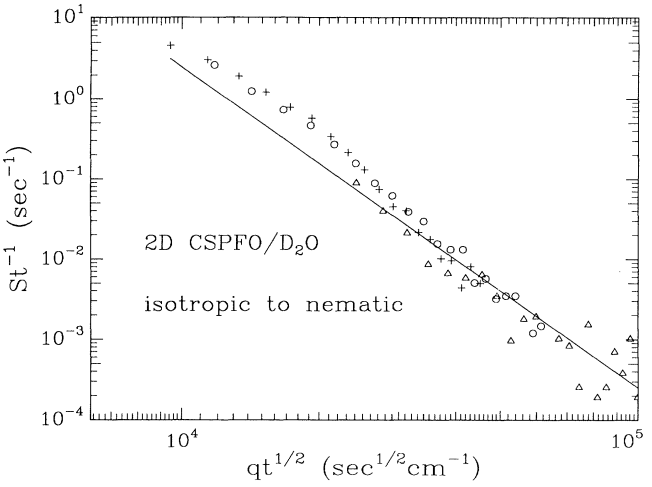

FIG. 9. Scaled form of 2D CsPFO data in the nematic region. The pluses, circles, and triangles are data at 240, 375, and 785 s after the quench, respectively. The solid line shows the fitted line at the high-q regime with a slope of -4.0.

follows from the generalized structure factor $S(q,t) \sim L(t)^d f(qL(t))$ with the result that $L(t) \sim t^{1/2}$. The results of 235, 501, and 2097 s after the quench all collapse onto this scaling curve. According to the generalized Porod law, the asymptotic slope of such a scaling curve will be $-(d+n)$. The slope of the solid line shown is -6.0 ± 0.3, which is consistent with $d=3$ and $n=3$.

Similar to PBLG-PBDG system, the time dependence of the coarsening of the length scale is shown in Fig. 8 as an A^* versus time plot. The slope of the straight line is -1.4 ± 0.2, confirming the $t^{1/2}$ growth of the length scale.

To study the 2D crossover behavior of the CsPFO, a wedgelike sealed cell was built with commercial grade quartz. The area of the cell accessible to light-scattering

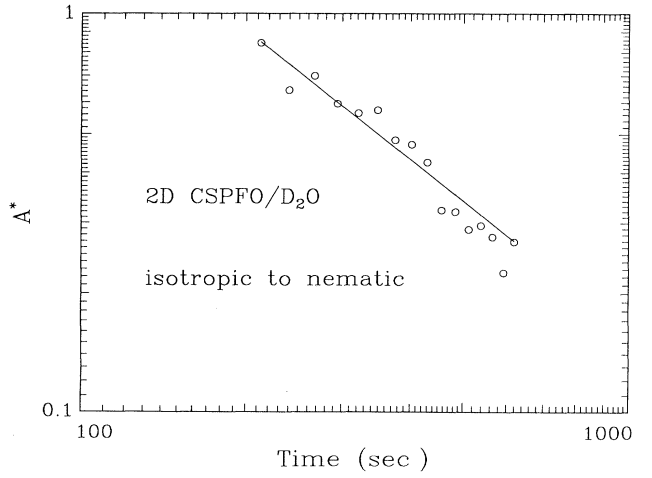

FIG. 10. Amplitude of -4 power-law fit (A^*) vs time for 2D CsPFO. The solid line is a fit with slope -1.1.

experiments allowed us to study the sample at thicknesses varying from 95 to 400 μm. The sample was found to display 2D behavior at a thickness of 100 μm and 3D behavior at thicknesses larger than 250 μm.

Figure 9 shows the scattering results at 100 μm at 240, 375, and 785 s after the quench in the scaled form of $S(q)t^{-1}$ versus $qt^{-1/2}$. As in the 3D case, the asymptotic slope of such a scaled curve is shown by the solid line, but in this 2D case the slope is -4.0 ± 0.3, which is consistent with $d=2$ and $n=2$.

The time dependence of the length scale growth is shown in Fig. 10 in the form of A^* versus time. The solid line is a fit with a slope of -1.1 ± 0.2. This is again consistent with the $t^{1/2}$ growth law.

DISCUSSION AND CONCLUSIONS

The two systems studied here are very different in many respects. PBLG-PBDG forms long rods while CsPFO forms disklike micelles. The width of the region of coexistence between isotropic and nematic phases spans almost 40 °C for PBLG, while it is only 0.5 °C wide for CsPFO. Moreover, the time scales at which the systems enter their scaling regime are very different: in the PBLG-PBDG system, the scaling regime occurs tens of hours after quenching while for CsPFO it starts at hundreds of seconds after the quench. However, remarkably, in spite of these differences, both systems display similar scaling behavior of the coarsening after they have been quenched from the isotropic into the nematic region of the phase diagram. This leads us to believe that our results are generic to quenched liquid-crystalline systems. When domains of isotropic and nematic material coexist we observe $q^{-(d+1)}$ power-law tails for large values of q in both three and two dimensions. This has been well understood as originating from the scattering of the domain walls. To our knowledge, the experiments in two dimensions are the first to show this behavior. When viewed under crossed polarizers, the domains are large compared to the cell thickness (50 and 100 μm, respectively) making them effectively two dimensional.

Both systems show $S(q) \sim q^{-6}$ in three dimensions and q^{-4} in two dimensions when quenched from the isotropic into the nematic region of the phase diagram. If we take the theoretical predictions [5,6] based on the n-vector model at face value our experiments suggest that $n=3$ in three dimensions and $n=2$ in two dimensions. It is important to realize, however, that for a nematic liquid crystal the order parameter is actually a traceless second-rank tensor. There is no direct mapping of a tensor order parameter onto a vector model. It is natural at this point to ask about the dominant source of scattering and the nature of the lengths scales involved. Since a nematic phase has continuous symmetry there are no domain walls in the ordered state that could be a source of scattering. The only singularities present are defects which can be point or line defects and textures. It is commonly accepted that the dominant defects in nematics are half-integer disclinations. In a recent series of experiments [14] small-angle light-scattering experiments

were performed on a polymer liquid crystal. The authors report two observations that we cannot confirm. First, they claim that the depolarized scattering pattern has four fold symmetry. Second, the patterns have a maximum at a finite value of q. Our scattering patterns are always azimuthally isotropic for nematic samples. For more highly ordered phases such as smectic ones, we do observe twofold and fourfold symmetries. The second claim, that the scattering patterns have a maximum at a finite value of q, is explained [14] using a model of interacting disclinations, where the length scale reflected by the maximum in $S(q)$ is given by an average distance between disclinations. We do agree with the idea that the dominant length scale in the system is related to the distance between disclinations and that the growth of this length scale is due to annihilation of two disclinations of opposite sign. This length scale is most certainly much larger than the "molecular" sizes (length of the PBLG rods or size of the CsPFO micelle) and can easily grow to hundreds of micrometers. This explains why we were able to observe crossover between two- and three-dimensional behavior at these large cell thicknesses. Since we do not observe a peaked structure factor, we must conclude that in our case the diclinations are not correlated and do not have a characteristic distance.

We calculated the scattering of disks with $s=1$ and $\frac{1}{2}$ disclinations and the associated director field based on formulas derived in Ref. [14]. We found that the scattering from such disks has indeed a power-law tail falling off with a slope of -4. This is what we observed for the two-dimensional nematic liquid crystals and indicates that the dominant defects here are stringlike defects stretching from one glass window to the opposite. The defects induce director fields akin to the 2D XY model, which is formally described by a two-vector model in two dimensions. In the calculations the size of the disks was irrelevant. The large-q behavior was caused solely by the scattering from the director field in the vicinity of the disclination.

Unfortunately the formulas for three-dimensional disclinations are not available. By analogy, however, we must conclude that the dominant source of scattering is also in this case the disclinations. It would be natural to conclude that this should be akin to the 3D XY model with $n=2$, which is in contradiction to our experimental results $n=3$. We must reiterate, however, that to the best of our knowledge there is no rigorous derivation of the value of n for a nematic phase. Only heuristic arguments [11] have been recently proposed that lend justification for $n=3$ for a nematic liquid crystal. A full tensor theory is awaited to which our data could be compared.

ACKNOWLEDGMENTS

We would like to thank G. Aeppli, A. J. Bray, N. Goldenfeld, T. C. Halsey, D. A. Huse, F. Liu, G. F. Mazenko, C. A. Murray, D. R. Nelson, and T. A. Witten for stimulating and constructive discussions. We also want to thank M. Marcus for his valuable assistance.

[1] P. Debye, H. R. Anderson, Jr., and H. Brumberger, J. Appl. Phys. **28**, 679 (1957).

[2] See, for example, G. Porod, in *Small-Angle X-Ray Scattering,* edited by O. Glatter and O. Kratsky (Academic, New York, 1982).

[3] F. S. Bates and P. Wiltzius, J. Chem. Phys. **91**, 3258 (1989), and references therein.

[4] See R. Bruinsma and G. Aeppli, Phys. Rev. Lett. **52**, 1547 (1984); R. J. Birgeneau, R. A. Cowley, G. Shirane, and H. Yoshizawa, J. Stat. Phys. **34**, 817 (1984), and references therein.

[5] A. J. Bray and S. Puri, Phys. Rev. Lett. **67**, 2670 (1991).

[6] F. Liu and G. F. Mazenko, Phys. Rev. B **45**, 6989 (1992).

[7] N. Boden, P. H. Jackson, M. McMullen, and M. C. Holmes, Chem. Phys. Lett. **65**, 476 (1979).

[8] W. G. Miller, C. C. Wu, E. L. Wee, G. L. Santee, J. H. Rai, and K. G. Goebel, Pure Appl. Chem. **38**, 37 (1974).

[9] M. C. Holmes, D. J. Reynolds, and N. Boden, J. Phys. Chem. **91**, 5257 (1987).

[10] A. Cumming, P. Wiltzius, F. S. Bates, and J. H. Rosedale, Phys. Rev. A **45**, 885 (1992).

[11] A. P. Y. Wong, P. Wiltzius, and B. Yurke, Phys. Rev. Lett. **68**, 3583 (1992).

[12] See, for example, M. Mondello and N. Goldenfeld, Phys. Rev. A **42**, 5865 (1990); H. Toyoki and K. Honda, Prog. Theor. Phys. **78**, 237 (1987); I. Chuang, N. Turok, and B. Yurke, Phys. Rev. Lett. **66**, 2472 (1991); M. Mondello and N. Goldenfeld, Phys. Rev. A **45**, 657 (1992).

[13] H. Toyoki, Phys. Rev. A **42**, 911 (1990), and references therein.

[14] T. Hashimoto, A. Nakai, T. Shiwaku, H. Hasegawa, R. Rojstaczer, and R. S. Stein, Macromolecules **22**, 422 (1989); T. Shiwaku, A. Nakai, H. Hasegawa, and T. Hashimoto, *ibid.* **23**, 1590 (1990).